doi: 10.34172/bi.2022.23393
http://bi.tbzmed.ac.ir/

Simulation and fabrication of an integrating well-aligned silicon nanowires substrate for trapping circulating tumor cells labeled with Fe_3O_4 nanoparticles in a microfluidic device

Vahid Ghafouri[*], Majid Badieirostami[1], Morteza Fathipour[1]

MEMS and NEMS Laboratory, School of Electrical and Computer Engineering, University of Tehran, Tehran, Iran

Supplementary file 1

In Fig. S1, the magnetic flux density norm is simulated in two dimensions (2D) in terms of positions in the microfluidic channel. Fig. S1(a) shows the entire magnet (the size of the magnet is approximate) in the part of the microfluidic channel that contains the microposts as well as the Si nanowires (SiNWs) substrate. Fig. S1(b) shows the magnetic flux density norm near the channel with higher magnification. Fig. S1(c) shows the magnetic flux density norm in terms of the horizontal coordinate (x) along the different vertical distances (y) inside the microfluidic channel that includes the microposts and the SiNWs substrate. As expected, when the vertical distance (y) increases, the field strength decreases, and the maximum field strength is related to the two ends of the magnet. Fig. S1(d) shows the magnetic flux density norm in terms of the vertical coordinate (y) along the different horizontal distances (x) with 100 μm spacing. The point to consider is that the drop in the field strength along the y-coordinate around the corners of the magnet is greater than the drop in its middle part.

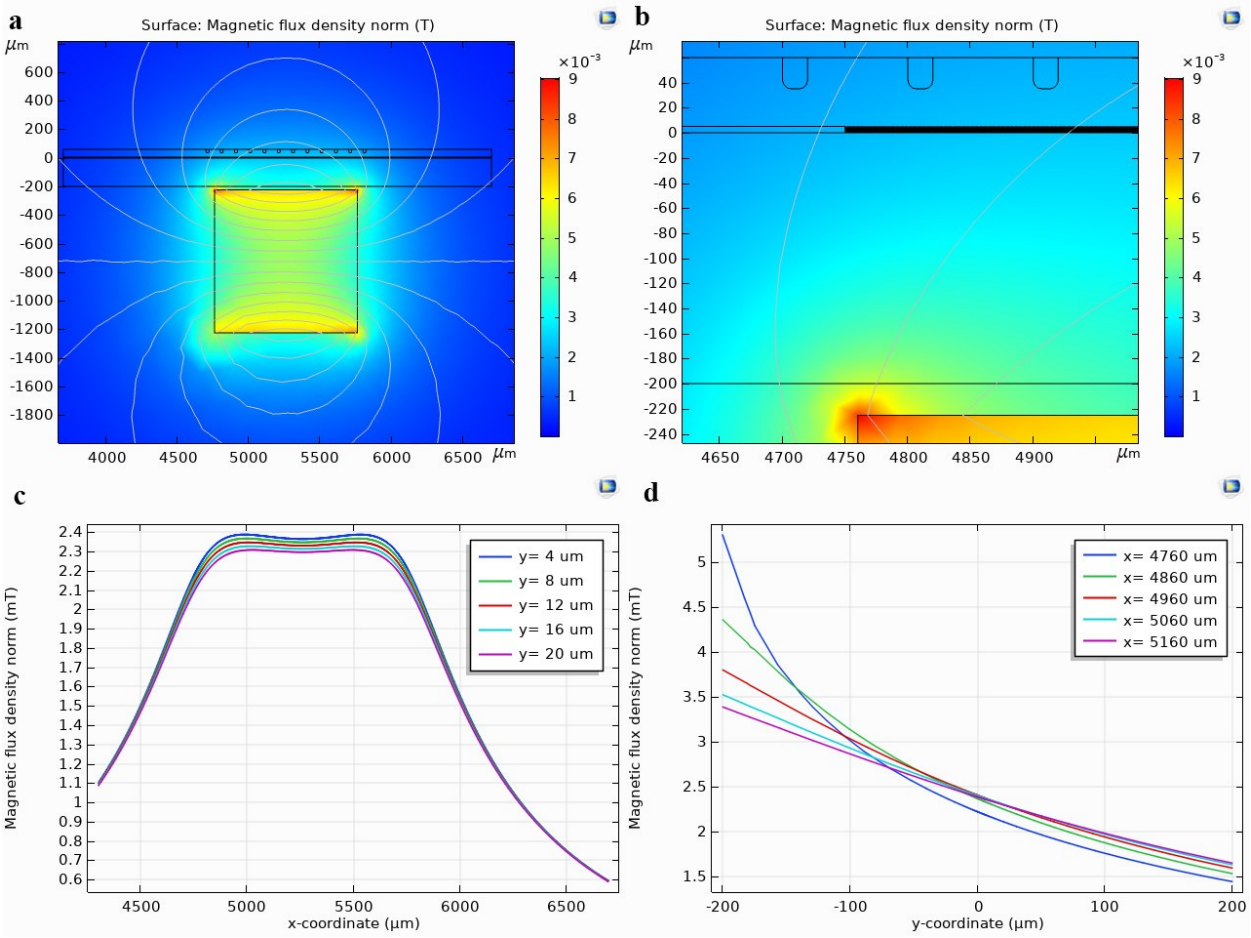

Figure S1. The magnetic flux density norm is simulated in 2D in terms of positions in the microfluidic channel. (a) The entire magnet located in the part of the microfluidic channel that contains the microposts as well as the SiNWs substrate. (b) The magnetic flux density norm near the channel with higher magnification. (c) The magnetic flux density norm in terms of the horizontal coordinate (x). (d) The magnetic flux density norm in terms of the vertical coordinate (y).

Fig. S2 indicates the 2D simulation of the fluid velocity (blood cells and buffer) in the microfluidic channel around the microposts and the nanowires substrate. Fig. S2(a) shows the lateral view of the fluid velocity around the microposts and their effect on the fluid flow. As can be seen, the presence of the microposts causes a periodic movement during fluid flow around the nanowires substrate. Another role that these microposts play in the movement of blood cells and CTCs is that they act as a barrier and cause these cells to be pulled down, allowing them to be trapped by the magnetophoretic force and the nanowires substrate. Fig. S2(b) shows a magnified view of a single micropost in the vicinity of the nanowires substrate. Figs. S2(c) and (d) show the magnitudes of the 1D velocity profile in terms of the horizontal coordinate (x) and for different distances from the nanowires substrate. Fig. S2(c) shows the fluid velocity for y = 5 μm exactly on the above the surface of the nanowires. For maximum distances from the nanowires substrate,

the peak velocity of the fluid is maximized at the intervals between the two microposts, and this peak shows an increase for different values of the vertical distance from the substrate until about 15 μm. Fig. S2(d) shows the changes in the velocity profile of fluid with increasing vertical distance from the substrate. For y = 20 μm, the peak velocity includes a notch. The drop in fluid velocity at y = 25 μm is much more pronounced due to the collision of the fluid with the micropost. Similarly, the velocity of the fluid decreases with increasing vertical distance, until finally at a distance of 35 μm, the velocity of the fluid from the sinusoidal shape tends to be tangential.

The fluid encounters two obstacles along the channel. One is the SiNWs embedded in the bottom of the channel and the other is the microposts. The cell has free movement until it hits the sidewalls and barriers such as the microposts embedded in the middle part of the channel. The Navier-Stokes fluidic force pushes the cell to move forward in the microfluidic channel. As seen in Fig. S2, the microposts act in such a way that the cells are pulled toward the substrate and are more likely to be trapped by the nanowires. As shown in Fig. S2, although the fluid velocity increases below the microposts, the cells will fall further due to their morphologies and their dimensions at this location. Another point is that, given the size of the RBCs and their morphologies, we expect them not to be trapped in this way.

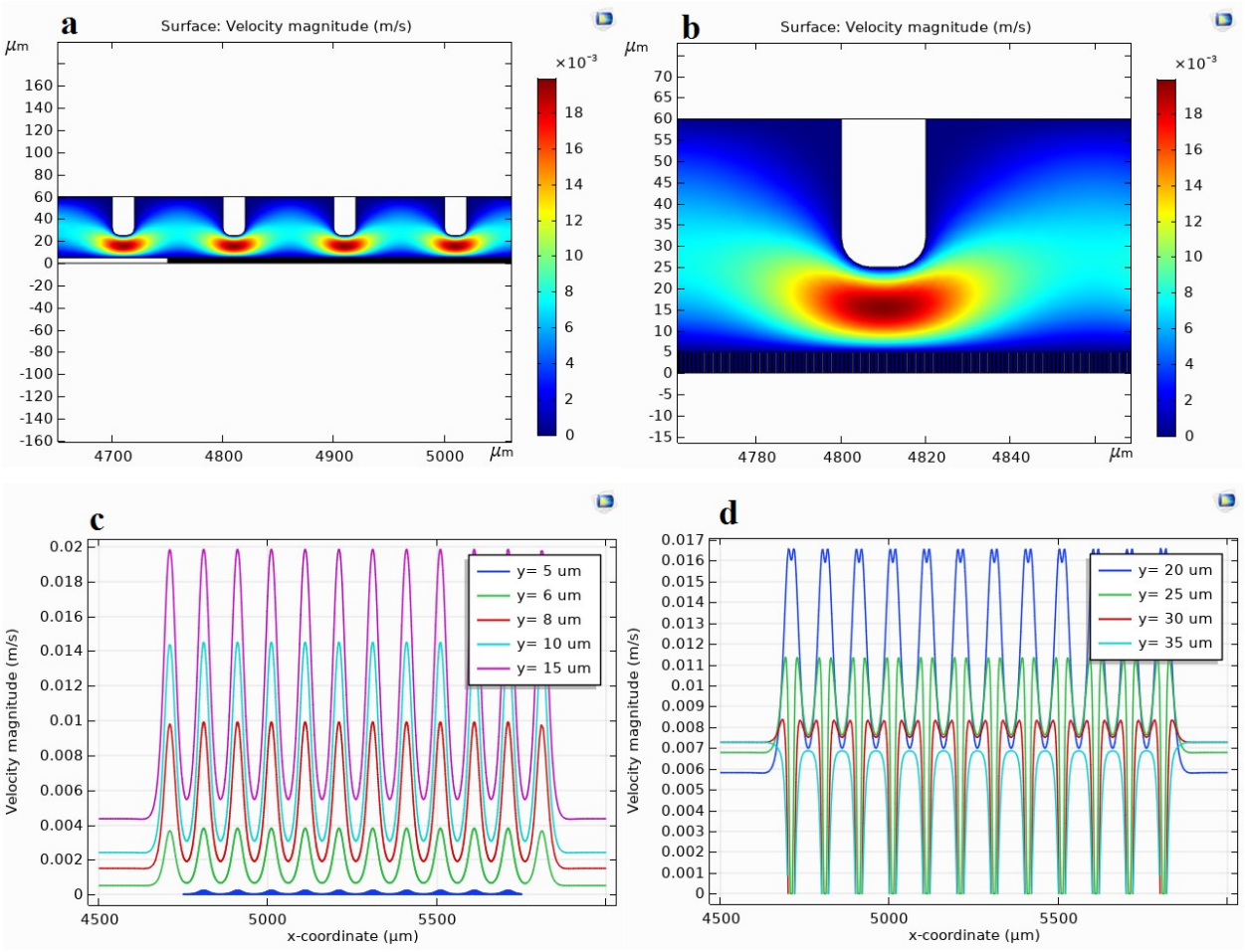

Figure S2. The 2D simulation of the fluid velocity (blood cells and buffer) in the microfluidic channel around the microposts and the nanowires substrate. (a) The lateral view of the fluid velocity around the microposts and their effect on the fluid flow. (b) A high magnification view of a single micropost in the vicinity of the nanowires substrate. (c-d) The magnitudes of the 1D velocity profile in terms of horizontal coordinate (x) and for different distances from the nanowires substrate.

In Movie S1, the motion of two different types of particles is examined under the influence of the magnetophoretic force and in the presence of the nanowires substrate as well as the microposts. In this simulation, we considered the larger particles to be the same size as the CTCs and the smaller particles to be the same size as the WBCs.

Fig. S3(a) indicates the EDX analysis of a sample of the silica-coated PMNPs shown in Figure 3. As seen in this figure, the oxygen and iron peaks are related to the nanoparticles and the silicon peaks are related to the substrate. Table S1 shows the elemental analysis of each component in the substrate with iron oxide nanoparticles. The hysteresis loops measured for the non-coated and the silica-coated magnetite nanoparticles are presented in Fig. S3(b). For both samples the non-zero coercive fields and the remanence values were measured.

Table S1. Elemental analysis of each element in the substrate with PMNPs.

Element	Weight %	Atomic %	Net Int.	Error %	K_{ratio}
OK	46.9	64.5	39.6	10.6	0.1529
SiK	37.1	29.1	103.7	6.9	0.2145
FeK	16.0	6.3	21.2	8.0	0.1361

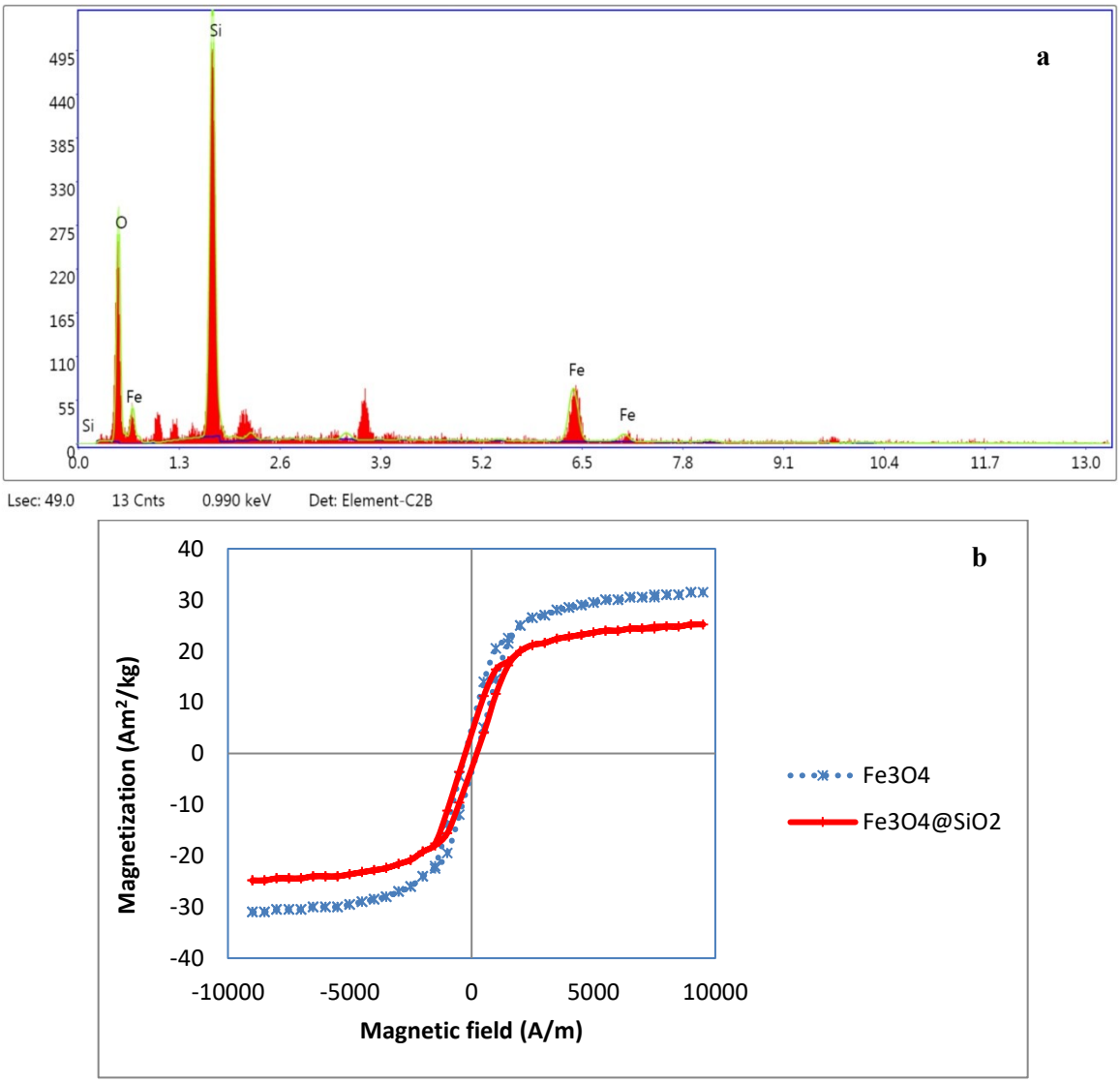

Figure S3. (a) EDX analysis of the silica-coated PMNPs. As seen in this figure, the oxygen and iron peaks are related to the nanoparticles and the silicon peaks are related to the substrate. (b) Magnetic hysteresis loops measured for the noncoated and the silica-coated Fe_3O_4 nanoparticles.

Fig. S4(a) shows a schematic process of photolithography and fabrication of well-aligned SiNWs substrate. After developing a microfluidic channel using a conventional lithography process on a silicon substrate, we used a surface patterning process with silver nanoparticles and the use of wet etching to fabricate nanowires substrate in the channel. The process of placing nanoparticles on a non-resistive positive site and how to remove the nanoparticles is completely illustrated in the schematic layout. Fig. S4(b) schematically illustrates the soft lithography process for fabricating the microfluidic channel. Using a negative photoresist, a mold is designed to replicate the reverse of the previously designed SiNWs substrate shape and set the microfluidic channel at height of 50 μm.

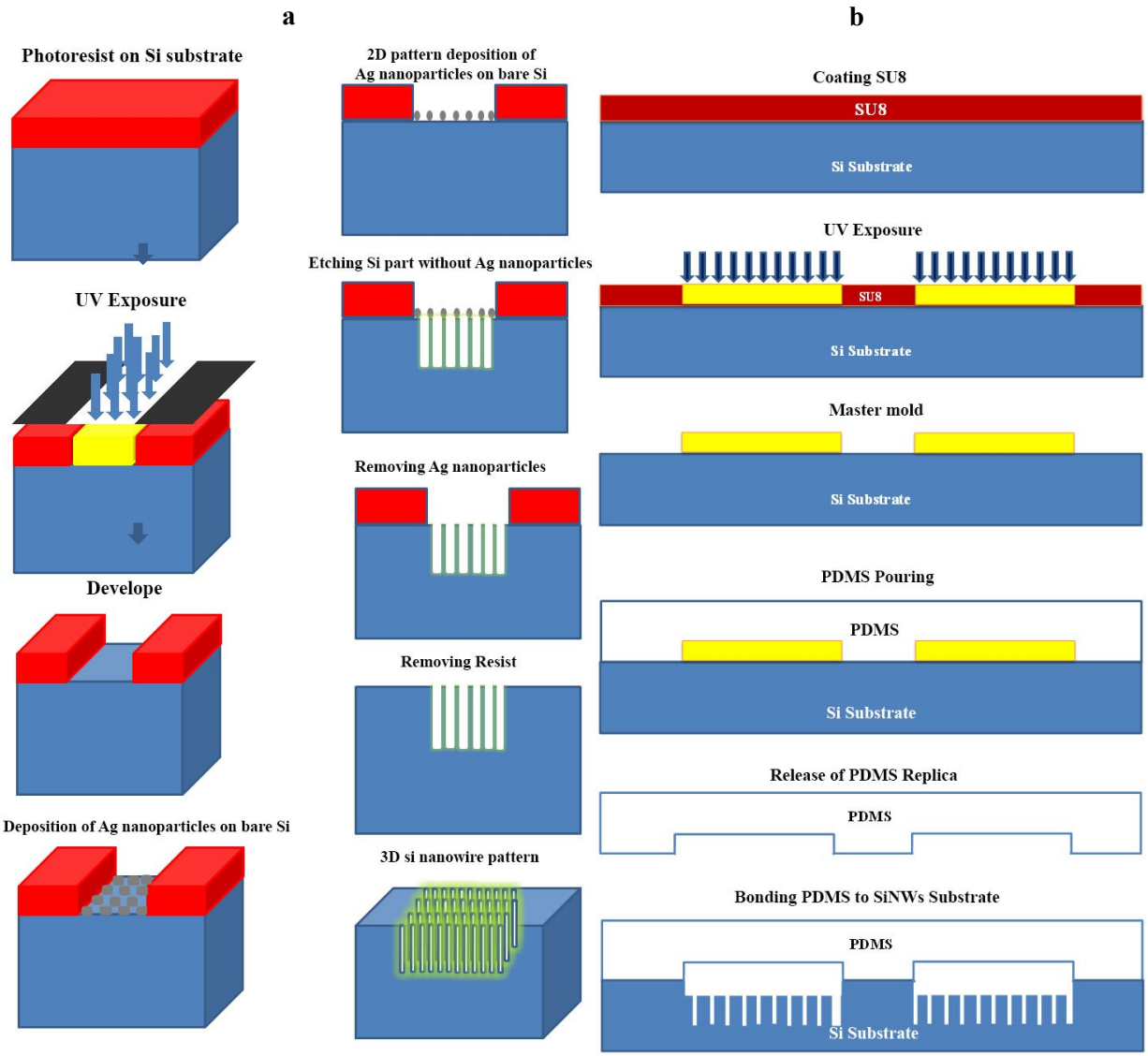

Figure S4. (a) Schematic process of photolithography and fabrication of well-aligned SiNWs substrate. (b) Schematic of the soft lithography process for the microfluidic channel fabrication.